Research Square

Preprints are preliminary reports that have not undergone peer review.
They should not be considered conclusive, used to inform clinical practice,
or referenced by the media as validated information.

Sixteen-year tuberculosis notification trends, spatial heterogeneity, treatment outcomes and diagnostic delay in Khuzestan, Iran: a registry-based study

Shokrollah Salmam Zadeh
Ahvaz Jundishapur University of Medical Sciences
Neda Kaydi
Ahvaz Jundishapur University of Medical Sciences
Morteza Abdullatif Khafaie
m.khafaie@live.com
Ahvaz Jundishapur University of Medical Sciences
Nematallah Jaafarzadeh
Ahvaz Jundishapur University of Medical Sciences

Research Article

Keywords: tuberculosis, disease surveillance, spatial epidemiology, diagnostic delay, treatment outcome, administrative boundaries, Iran

Posted Date: September 21st, 2026

DOI: https://doi.org/10.21203/rs.3.rs-10778311/v1

License: This work is licensed under a Creative Commons Attribution 4.0 International License.
Read Full License

Additional Declarations: No competing interests reported.

Abstract

Background

Long-term subnational tuberculosis (TB) surveillance can be biased when administrative boundaries and population denominators change over time. We examined temporal, geographic and clinical patterns of TB in Khuzestan, Iran, using a harmonised framework designed to preserve numerator-denominator comparability across a 16-year surveillance period.

Methods

This retrospective registry-based study included 9,090 TB registration episodes from 16 Persian-calendar surveillance years, presented as corresponding Gregorian intervals (2005–06 to 2020–21). Rates across 20 harmonised historical county groups were descriptive. Longitudinal and grid analyses were restricted to 6,047 residence-based new-and-relapse episodes in 10 historical units with continuously comparable surveillance coverage. Census-anchored populations were reconstructed for non-census years. Negative-binomial population-offset models estimated annual percentage change; empirical-Bayes rates and spatial autocorrelation assessed geographic patterning. Modified Poisson and median regression assessed adverse treatment outcomes and diagnostic delay.

Results

The model-standardised age-adjusted notification rate declined by 2.67% per year (95% CI − 3.55 to − 1.77). Pooled crude notification rates across the 20 historical county groups ranged from 1.77 to 22.64 per 100,000 person-years. Global spatial autocorrelation in the primary 10-km grid was modest (Moran's I = 0.0648; permutation P = 0.0344), and none of 432 local tests remained significant after false-discovery-rate correction. Adverse outcomes occurred in 944/8,718 eligible episodes (10.8%). Median diagnostic delay among 9,058 nonnegative intervals was 55 days (IQR 30–94), with a 95th percentile of 322 days.

Conclusions

TB notifications declined, but geographic heterogeneity and substantial diagnostic delay persisted. Harmonising historical geography separated province-wide description from stronger longitudinal and spatial inference and may be useful in other long-term surveillance settings affected by administrative change. The absence of false-discovery-rate-supported local clusters cautions against interpreting isolated high-rate cells as confirmed hotspots. Findings support targeted programme review but do not establish causal effects.

Background

Tuberculosis (TB) remains a major infectious cause of morbidity and mortality worldwide, and gaps persist between estimated disease burden and the cases diagnosed and notified to health systems [1]. Notification data are central to programme monitoring, but notification rates are not direct measures of disease incidence: they reflect underlying disease occurrence together with access to care, diagnostic practice, case finding, recording and reporting. Evaluations of the Iranian surveillance system have documented underascertainment, underreporting and limitations in timeliness, reinforcing the need for cautious interpretation of notification-based estimates [2, 3].

Long-term subnational surveillance introduces an additional comparability problem. Changes in administrative boundaries or surveillance coverage can create numerator-denominator mismatch, while population growth and changing age structure can alter crude rates independently of disease occurrence. National analyses in Iran have generally indicated declining TB trends, although estimates differ by case definition, period and data source [4, 5]. A recent Global Burden of Disease 2021 analysis likewise reported a long-term decline in age-standardised TB incidence in Iran while showing substantial provincial variation [6]. These findings make geographic and denominator harmonisation important when interpreting long regional time series.

Spatial studies in Iran have identified geographic heterogeneity in TB at national, provincial and county scales [7–10]. Such studies provide important context, but administrative-area analyses do not answer the same question as residence-linked small-area analyses, and global spatial dependence does not imply that individual local clusters are statistically robust. Multiple local tests can also produce apparently significant areas by chance if multiplicity is not controlled. Alongside geographic surveillance, treatment outcomes and diagnostic delay provide complementary information on programme performance and care pathways. Evidence from Iran and the wider Middle East and North Africa shows that diagnostic delay varies substantially by population and care context [12–15], while current World Health Organization guidance emphasises timely diagnosis, treatment, follow-up and patient-centred care [16, 17].

Previous work from Khuzestan described TB trends during 2010–2019 [11], but did not jointly address historical administrative change, census-anchored denominator reconstruction, separation of province-wide descriptive geography from a fixed longitudinal domain, residence-linked fine-grid spatial analysis with multiplicity control, and episode-level treatment outcomes and diagnostic delay. The present study extends that evidence across 16 surveillance years. We aimed to characterise temporal trends in TB notification, geographic and fine-scale spatial heterogeneity, adverse treatment outcomes and diagnostic delay, and their associated characteristics, while explicitly preserving the distinction between descriptive notification patterns and stronger longitudinal or spatial inference.

Methods

Study design, setting and populations

We conducted a retrospective registry-based observational study in Khuzestan Province, southwestern Iran. Sixteen Persian (Solar Hijri/Jalali) surveillance years were presented as corresponding Gregorian intervals from 2005–06 to 2020–21. These surveillance years span approximately March to March; records were not reassigned to January–December calendar years. The analytical unit was a TB registration episode because no validated identifier established unique persons across annual exports. All eligible registry records were included; no a priori sample-size calculation was performed. The registry contained 9,090 episodes. Treatment-outcome analyses included 8,718 eligible episodes. Diagnostic delay was defined as diagnosis date minus recorded symptom-onset date after validated calendar conversion. The interval was calculable for 9,060 episodes; two negative intervals were retained for data-quality assessment but excluded from inferential analyses, leaving 9,058 nonnegative intervals. Notification-rate and grid analyses used 6,047 residence-based new-and-relapse episodes in 10 surveillance units with continuously comparable coverage: Ahvaz, Omidiyeh, Andimeshk, Izeh, Bagh Malek, Dasht Azadegan, Ramshir, Ramhormoz, Lali and Masjed Soleyman. Treatment success comprised cure or treatment completion. The adverse-outcome endpoint comprised treatment failure, loss to follow-up or death; ongoing treatment, transfer, misdiagnosis and other nonclassifiable outcomes were excluded from the binary endpoint, leaving 372 episodes outside that analysis.

Geography, population denominators and temporal analysis

All 20 harmonised historical county groups, comprising 7,685 new-and-relapse episodes, were retained for pooled descriptive county-rate analysis. Because comparable numerator and denominator geography could not be established across all groups throughout the full period, longitudinal and spatial inference was restricted a priori to the 10 historically comparable surveillance units. These units were selected on the basis of historical surveillance and geographic comparability, not on observed TB rates.

Later administrative units were crosswalked to historical parent units where required. Population denominators were anchored to official census totals harmonised to the historical geography. Population values between census anchors were reconstructed using prespecified log-linear models, with limited endpoint extrapolation where necessary. Intermediate annual populations therefore represent modelled denominators rather than observed annual census counts and approximate population person-time over each surveillance interval.

WorldPop Global1 annual, unconstrained, non-UN-adjusted 1-km population surfaces for Iran [18] were used only to distribute each reconstructed unit-year population within the corresponding surveillance unit for grid analyses. Each surface was calibrated to the census-anchored reconstructed unit total. WorldPop therefore did not replace official population control totals and was not treated as an exposure variable.

The primary measure was the annual new-and-relapse TB notification rate per 100,000 population. Negative-binomial regression of episode counts, with log population as an offset, estimated annual percentage change (APC) as $100 \times [\exp(\beta) - 1]$, where β was the surveillance-year coefficient. Model-standardised age adjustment was the primary temporal analysis: counts and denominators were

stratified into 0–14, 15–64 and ≥ 65 years and standardised to the 2016–17 age distribution of the fixed surveillance domain. Direct age standardisation using the same age groups was used as a confirmatory analysis. Age-specific trends and exclusion of the final 2020–21 interval were supporting sensitivity analyses.

Spatial analysis

Residence linkage and spatial aggregation used a restricted geocoding workflow; no new geocoding was conducted for this manuscript, and addresses and exact coordinates were excluded from publication outputs. Study-period new-and-relapse episode counts and population person-time were aggregated to fixed analytical grids. The primary analysis used pooled empirical-Bayes-smoothed notification rates [19] for the 432 positive-population cells of the 10-km grid. Global spatial autocorrelation was assessed using Moran's I [20] with row-standardised rook-contiguity weights and 9,999 permutations. Local Moran statistics [21] were calculated for eligible cells, with multiplicity controlled using the Benjamini-Hochberg false-discovery-rate procedure [22]. Sensitivity analyses used crude rates and queen-contiguity weights. A nested 5-km grid was retained as a resolution-sensitivity analysis because greater sparsity reduced inferential stability; the 10-km analysis remained primary.

Clinical analyses

Modified Poisson regression with sandwich variance estimated adjusted risk ratios (aRRs) for adverse treatment outcomes. Prespecified covariates were age, sex, disease site, registration history and registration year. Because diagnostic delay was right-skewed, median regression ($\tau = 0.50$) estimated adjusted conditional median differences using the same covariates. Age was scaled per 10 years and registration year per year. Confidence intervals for median regression used Huber-sandwich standard errors with sparsity estimation in R quantreg version 6.1; kernel-based standard errors provided a concordance sensitivity analysis. Missing values were not imputed, and each model used its applicable denominator. Diagnostic delay represented the recorded symptom-onset-to-diagnosis interval and could not be partitioned into patient and health-system components. Same-day intervals were coded as zero. Negative intervals were excluded from inferential analysis as described above; long positive intervals were retained without truncation or winsorisation. Current incarceration at registration was examined only as a post hoc secondary analysis. Analyses were conducted in validated Python and R environments and interpreted as observational associations, not causal effects. Reporting followed the STROBE recommendations [23].

Use of AI-assisted tools

OpenAI ChatGPT was used as an assistive tool for coding support, and Paperpal was used for language editing. All scientific content, analyses, interpretations and conclusions were reviewed and verified by the authors.

Results

Registry population and analytical cohorts

The registry comprised 9,090 registration episodes, with age data available for 9,085 episodes. Among 8,718 outcome-eligible episodes, 7,774 (89.2%) resulted in treatment success and 944 (10.8%) had adverse outcomes. The fixed 10-unit longitudinal and grid cohort included 6,047 residence-based new-and-relapse episodes (Table 1). Among 9,058 nonnegative diagnostic-delay intervals, the median delay was 55 days (IQR 30–94).

Table 1
Registry characteristics and analytical denominators

Characteristic	n/N	Summary
Age, years	9085/9090	40.5 (18.0); 36 (27–53)
Male sex	5456/9090	60.0%
Pulmonary TB	6776/9090	74.5%
New registration	8286/9090	91.2%
Relapse	387/9090	4.3%
Current incarceration at registration (post hoc secondary)	915/9090	10.1%
Treatment success	7774/8718	89.2%
Adverse treatment outcome	944/8718	10.8%
Diagnostic delay, days	9058/9090	55 (30–94)
Primary rate/spatial cohort	6047/9090	Residence-based new-and-relapse episodes

Values are expressed as n/N (%) unless otherwise indicated. Age is reported as mean (SD) and median (IQR), and diagnostic delay is reported as median (IQR). Treatment outcomes were based on 8718 outcome-eligible episodes. Diagnostic delay uses 9058 non-negative intervals. Current incarceration was a post hoc secondary characteristic. Registry records are registration episodes, not verified unique persons. IQR, interquartile range; SD, standard deviation; TB, tuberculosis.

Temporal trends

The crude new-and-relapse notification APC was − 2.24% per year (95% CI − 3.33 to − 1.14), while the primary model-standardised age-adjusted APC was − 2.67% per year (95% CI − 3.55 to − 1.77). The directly age-standardised APC was − 2.62% per year (95% CI − 3.89 to − 1.33) (Fig. 1; Table 2). Age-specific APCs were − 3.50% per year (95% CI − 7.01 to 0.13) among those aged 0–14 years, − 2.37% (95% CI − 3.44 to − 1.28) among those aged 15–64 years and − 3.20% (95% CI − 5.05 to − 1.31) among those aged ≥ 65 years. Excluding the final interval (2020–21), the crude APC remained negative at − 1.48% per year (95% CI − 2.35 to − 0.59).

Table 2. Temporal, geographic and spatial patterns of new-and-relapse TB notification

A. Temporal trends

Analysis	Measure	Estimate (95% CI where applicable)
Crude notification trend	APC, %/year	−2.24 (−3.33 to −1.14)
Model-standardised age-adjusted trend	APC, %/year	−2.67 (−3.55 to −1.77)
Directly age-standardised trend	APC, %/year	−2.62 (−3.89 to −1.33)
Age 0–14 years	APC, %/year	−3.50 (−7.01 to 0.13)
Age 15–64 years	APC, %/year	−2.37 (−3.44 to −1.28)
Age ≥65 years	APC, %/year	−3.20 (−5.05 to −1.31)
Excluding the final surveillance interval (2020–21)	Crude APC, %/year	−1.48 (−2.35 to −0.59)

B. Geographic variation

Analysis	Measure	Estimate (95% CI where applicable)
All 20 historical county groups	Pooled crude notification-rate range	1.77–22.64/100000 person-years
Fixed 10-unit longitudinal domain	Pooled directly age-standardised rate range	5.38–21.62/100000

C. Spatial autocorrelation

Analysis	Measure	Estimate (95% CI where applicable)
Primary 10-km empirical-Bayes field	Global Moran I	0.0648; permutation P = 0.0344
Local Moran, nominal P < 0.05	Cells	23/432
Local Moran, BH-FDR supported	Cells	0/432

APC, annual percentage change; BH-FDR, Benjamini–Hochberg false-discovery-rate correction; CI, confidence interval; TB, tuberculosis. Rates are notification rates. Primary temporal inference uses the fixed 10-unit continuously comparable domain; all 20 historical county groups are descriptive. Direct age standardisation used age bands 0–14, 15–64 and ≥65 years and the 2016–17 fixed-domain population as the internal standard. Surveillance intervals retain the underlying Persian-calendar structure and are presented by their Gregorian spans; counts were not redistributed to January–December years. Global

and Local Moran analyses used 9,999 permutations. The 23 nominal Local Moran cells are not confirmed clusters; none remained supported after BH-FDR correction.

Geographic and spatial patterns

Across 20 harmonised historical county groups, pooled crude notification rates ranged from 1.77 per 100,000 person-years in Shadegan to 22.64 per 100,000 person-years in Andimeshk; corresponding rates were 16.87 in Ahvaz and 14.48 in Ramhormoz (Fig. 2). Within the fixed 10-unit domain, directly age-standardised pooled rates ranged from 5.38 per 100,000 person-years in Lali to 21.62 per 100,000 person-years in Andimeshk. Crude and age-standardised rankings were highly concordant (Spearman ρ = 0.988; maximum rank shift, one position).

The primary 10-km analysis included 432 positive-population cells. Global Moran's I was 0.0648 (permutation P = 0.0344), indicating modest positive global spatial autocorrelation. Of 432 local Moran tests, 23 had nominal P < 0.05, but none remained statistically supported after Benjamini-Hochberg false-discovery-rate correction. The 5-km analysis, retained as a resolution sensitivity analysis, likewise provided no false-discovery-rate-supported evidence of local clustering (Fig. 2; Table 2).

Treatment outcome and diagnostic delay

Adverse outcomes were associated with male versus female sex (aRR 1.59, 95% CI 1.38–1.84), relapse versus new registration (aRR 1.38, 95% CI 1.09–1.74), other retreatment versus new registration (aRR 1.86, 95% CI 1.53–2.28), age (aRR 1.019 per 10 years, 95% CI 1.011–1.027) and later registration year (aRR 1.019 per year, 95% CI 1.005–1.034). Extrapulmonary TB had a lower observed risk of adverse outcomes than pulmonary TB (aRR 0.39, 95% CI 0.31–0.48) (Table 3). Adjusted conditional median diagnostic delay was 8.48 days shorter in male than female episodes (95% CI − 11.49 to − 5.48) and 13.97 days shorter for relapse than new registrations (95% CI − 16.56 to − 11.39). Delay was 16.76 days longer for extrapulmonary than pulmonary TB (95% CI 13.03–20.48) and 30.71 days longer for other retreatment than new registrations (95% CI 13.57–47.85). Age was associated with a 0.54-day increase in median delay per 10 years (95% CI 0.30–0.77), while the registration-year coefficient was − 0.26 days per year (95% CI − 0.57 to 0.04) (Table 3).

Table 3. Adjusted associations with adverse treatment outcome and diagnostic delay

A. Adverse treatment outcome

Characteristic	aRR	95% CI
Age, per 10 years	1.019	1.011 to 1.027
Male sex	1.59	1.38 to 1.84
Extrapulmonary TB	0.39	0.31 to 0.48
Relapse	1.38	1.09 to 1.74
Other retreatment	1.86	1.53 to 2.28
Registration year, per year	1.019	1.005 to 1.034

B. Diagnostic delay

Characteristic	Adjusted median difference, days	95% CI
Age, per 10 years	0.54	0.30 to 0.77
Male sex	−8.48	−11.49 to −5.48
Extrapulmonary TB	16.76	13.03 to 20.48
Relapse	−13.97	−16.56 to −11.39
Other retreatment	30.71	13.57 to 47.85
Registration year, per year	−0.26	−0.57 to 0.04

Post hoc secondary analysis

Characteristic	Adjusted estimate	95% CI
Current incarceration — adverse outcome	0.62	0.50 to 0.77
Current incarceration — diagnostic delay	−17.53	−20.32 to −14.75

Analytical N=8718 for adverse treatment outcome (944 adverse events) and N=9058 for diagnostic delay. Reference categories are female sex, pulmonary TB, new registration, and not currently incarcerated. Age estimates are per 10-year increase; registration-year estimates are per one surveillance-year increase. Adverse-outcome estimates are adjusted risk ratios from modified Poisson regression. Delay estimates are adjusted median differences from median regression; confidence intervals used a Huber-sandwich standard-error procedure with local sparsity estimation. Current-incarceration estimates are post hoc secondary observational analyses and must not be interpreted as protective or beneficial. aRR, adjusted risk ratio; CI, confidence interval; TB, tuberculosis.

Diagnostic delay was strongly right-skewed: the 90th, 95th and 99th percentiles were 193, 322 and 730 days, respectively. A total of 303 intervals exceeded one year and 86 exceeded 730 days. Validated

residence linkage was available for 8,063 of 9,058 delay episodes (89.02%).

Post hoc incarceration analysis

Current incarceration at registration was recorded in 915 of 9,090 episodes (10.1%); 902 of 915 episodes (98.6%) involved men. In post hoc analyses, incarceration was associated with a lower observed risk of adverse outcomes (aRR 0.62, 95% CI 0.50–0.77) and a 17.53-day shorter adjusted conditional median diagnostic delay (95% CI − 20.32 to − 14.75).

Discussion

Principal findings

Across a 16-year registry period, TB notification declined in the historically comparable surveillance domain, and the decline remained after adjustment for modelled population age structure and in supporting sensitivity analyses. Geographic heterogeneity was substantial, but the spatial signal was limited to modest positive global autocorrelation: no local cluster remained statistically supported after false-discovery-rate correction. Adverse outcomes occurred in approximately one in nine outcome-eligible episodes. Median diagnostic delay was 55 days and concealed a pronounced upper tail, with 5% of calculable episodes exceeding 322 days. Outcome and delay patterns varied by sex, disease site and registration history, but these registry associations do not establish causal mechanisms.

Interpretation

The similarity of crude and age-adjusted trend estimates indicates that changes in modelled age composition alone did not explain the decline in notifications. National Iranian studies have also reported decreasing or segmented TB trends [4, 5], and a recent Global Burden of Disease 2021 analysis reported declining age-standardised incidence alongside marked provincial disparities [6]. Nevertheless, registry notification reflects disease occurrence together with access to care, case finding, diagnostic practice and reporting completeness [2, 3]; our notification rates should therefore not be interpreted as direct estimates of incidence. The negative trend also persisted when 2020–21 was excluded, reducing the likelihood that the result was driven solely by the final surveillance interval. That interval still warrants caution because Iranian studies have documented COVID-19-related disruption of TB diagnosis and detection [24].

The separation of province-wide descriptive geography from a fixed 10-unit longitudinal domain is central to interpretation. All 20 harmonised historical county groups provide useful geographic context, whereas the fixed domain preserves comparable numerator and denominator geography across the full period. Within that domain, Andimeshk had the highest age-standardised pooled notification rate, and the near-identical crude and standardised rankings suggest that broad age-structure differences had little influence on geographic ordering. Previous Iranian studies at national, provincial and county scales have also reported spatial heterogeneity [7–10]. However, differences in service access, referral

pathways, case finding, reporting and population composition may all contribute to notification geography; the maps should not be read as causal or transmission hierarchies.

The spatial findings further illustrate why global and local statistics should be distinguished. Moran's I identified weak but detectable overall similarity among neighbouring cells, while none of 432 local tests survived false-discovery-rate correction. These findings are compatible rather than contradictory: a modest global tendency towards spatial similarity can exist without any single local cluster having sufficiently strong evidence after accounting for multiple testing. The stability of this interpretation across resolution and contiguity sensitivity analyses, together with residual uncertainty from residence geocoding and sparse fine-grid counts, argues against labelling isolated high-rate cells as confirmed hotspots.

Male sex and previous treatment history were associated with adverse outcomes, consistent with earlier Iranian registry studies in which demographic, clinical and treatment-history characteristics influenced unfavourable outcomes [25–27]. More recent survival analyses from southeastern Iran similarly highlight heterogeneity in prognosis across patient characteristics and care contexts [28]. In our data, extrapulmonary TB was associated with a lower observed adverse-outcome risk than pulmonary TB; this may reflect case mix, ascertainment or treatment-pathway differences and should not be interpreted as a protective effect. Current WHO guidance emphasises effective treatment, follow-up and patient support [17], but the present observational associations cannot identify which intervention would alter outcome risk.

Diagnostic delay adds a complementary view of care pathways. The median of 55 days is close to the national Iranian estimates reported by Nasehi and colleagues, who also observed longer delays among women and shorter delays among prisoners [14]. A systematic review from the Middle East and North Africa identified substantial heterogeneity in delay and reported associations with age, sex and socioeconomic factors [12], while a broader high-burden-country review likewise documented wide variation in definitions and determinants [13]. Recent large-scale surveillance work in China further demonstrates that diagnostic delay reflects both individual characteristics and health-service context [15]. The long right tail in our data is therefore programmatically important because a median alone conceals a smaller group experiencing very prolonged intervals. Longer adjusted delay among extrapulmonary episodes is clinically plausible given the diagnostic complexity of extrapulmonary presentations [16, 29]. However, the registry lacked organ-specific information, care-seeking sequences and separate patient- and health-system-delay components, so these mechanisms could not be tested.

The shorter adjusted delays observed among men, relapse episodes and currently incarcerated episodes should not be interpreted as evidence of benefit. The incarceration analysis was post hoc, incarceration was overwhelmingly concentrated among men, and no prison-population denominator was available. The shorter delay is consistent with earlier Iranian surveillance data reporting shorter diagnostic intervals among prisoners [14], but that pattern may reflect screening intensity, referral processes or selection. Conversely, recent survival analyses in southeastern Iran underline that incarceration-related

prognostic patterns depend on outcome definition and setting [28]. Our registry cannot estimate prison-specific TB incidence or transmission, nor the causal effect of incarceration on access to care.

Strengths and limitations

Strengths include the 16-year registry period; explicit separation of analytical cohorts and estimands; harmonisation of historical geography; census-anchored population reconstruction; age adjustment; residence-linked spatial analysis; empirical-Bayes stabilisation of small-area rates; correction for multiple local tests; resolution and contiguity sensitivity analyses; and disclosure-controlled publication outputs. The analytic design also distinguishes province-wide descriptive rates from the fixed historical domain used for stronger longitudinal and spatial inference, reducing the risk of drawing trend conclusions from geographically noncomparable numerator and denominator series.

Several limitations remain. Registration episodes could not be reliably linked to unique persons, so repeat registrations may have occurred. Notification patterns may reflect changes in case finding, diagnostic practice, service organisation or reporting completeness. Annual denominators between census anchors and at extrapolated endpoints were modelled rather than directly observed, and only broad age categories were available for standardisation. Residence geocoding has positional uncertainty, and residence linkage for diagnostic-delay analyses was incomplete. Symptom-onset dates may be affected by recall and recording error, while very long intervals may include data-quality uncertainty despite our decision to retain rather than arbitrarily truncate them. Clinical models may also be affected by residual confounding.

The adverse-outcome endpoint combines treatment failure, loss to follow-up and death, which may have different determinants. The delay measure could not distinguish patient delay from health-system delay. The incarceration analysis was post hoc and lacked a population denominator. Finally, the 20 historical county-group estimates are descriptive; the strongest longitudinal and spatial inferences apply to the reconstructed 10-unit domain with continuously comparable surveillance coverage. These limitations reinforce the use of the findings for surveillance review and hypothesis generation rather than causal attribution.

Conclusions

TB notifications declined over the study period, but substantial geographic heterogeneity persisted. Modest positive global spatial autocorrelation was not accompanied by any local cluster supported after false-discovery-rate correction. Adverse outcomes affected approximately one in nine eligible episodes, and diagnostic delays had a pronounced upper tail. The combination of historical geography harmonisation, census-anchored denominators and explicit separation of descriptive from inferential spatial analyses provides a transferable approach for long-term surveillance settings affected by administrative change. Programmatically, the findings support review of diagnostic pathways, particularly for extrapulmonary and other-retreatment episodes, and continued attention to follow-up

among previously treated patients. Spatial patterns are appropriate for prioritising surveillance review, not for defining confirmed hotspots or causal mechanisms without further local validation.

Abbreviations

TB
tuberculosis
APC
annual percentage change
aRR
adjusted risk ratio
BH-FDR
Benjamini-Hochberg false-discovery-rate correction
CI
confidence interval
EB
empirical Bayes
IQR
interquartile range
WHO
World Health Organization.

Declarations

Ethics approval and consent to participate

The study was approved by the Research Ethics Committee of Ahvaz Jundishapur University of Medical Sciences (IR.AJUMS.REC.1400.195; 19 June 2021). The requirement for informed consent was waived by the Research Ethics Committee. Analyses used restricted registry data and disclosure-controlled publication outputs; patient names, residential-address text and exact coordinates were not included.

Consent for publication

Not applicable. The manuscript contains no individual-level identifying information, images or other material requiring consent for publication.

Availability of data and materials

The WorldPop Global 1-km population surfaces used solely for within-unit spatial allocation are publicly available from WorldPop [18]. The individual-level TB registry data used and analysed in the current study

are not publicly available because they contain confidential health and residential-location information. De-identified, disclosure-controlled aggregate data and supporting analytical materials may be available from the corresponding authors upon reasonable request, subject to approval by the relevant institutional authorities and applicable data-governance requirements.

Competing interests

The authors declare that they have no competing interests.

Funding

The underlying TB research programme received institutional support from Ahvaz Jundishapur University of Medical Sciences through the Environmental Technologies Research Center (project no. 9402ETRC; tracking code 94423).

Authors' contributions

M.A.K. and N.K. conceived and designed the study, developed the methodology, curated and validated the data, conducted the statistical analyses, interpreted the findings, and contributed substantially to drafting and revising the manuscript. M.A.K. supervised the study, coordinated the project, and contributed to data visualisation and preparation of the figures. S.S.Z. contributed infectious-disease and clinical expertise, investigation, interpretation and validation of the findings, and drafting and critical revision of the manuscript. N.J. provided methodological and data-related advice, contributed to data interpretation and validation, and critically reviewed the manuscript. All authors read and approved the final manuscript and agree to be accountable for the work.

Acknowledgements

The authors gratefully acknowledge the Deputy for Health of Ahvaz Jundishapur University of Medical Sciences and the coordinator of the National Tuberculosis Control Program in Khuzestan Province for their valuable cooperation and support in facilitating access to the tuberculosis surveillance data used in this study.

References

1. World Health Organization. Global tuberculosis report 2025. Geneva: World Health Organization; 2025.
2. Kazerooni PA, Nejat M, Akbarpoor M, et al. Underascertainment, underreporting, representativeness and timeliness of the Iranian communicable disease surveillance system for tuberculosis and

brucellosis. Public Health. 2019;171:50–6. 10.1016/j.puhe.2019.03.008.

3. Bakhtiari A, Nasehi M, Rashidian A, et al. Evaluation of tuberculosis underreporting to National Tuberculosis Program (NTBP) based on data from laboratories in Tehran and NTBP. Med J Islam Repub Iran. 2019;33:70. 10.34171/mjiri.33.70.
4. Khazaei S, Soheilyzad M, Molaeipoor L, et al. Trend of smear-positive pulmonary tuberculosis in Iran during 1995–2012: a segmented regression model. Int J Prev Med. 2016;7:86. 10.4103/2008-7802.184317.
5. Arsang-Jang S, Mansourian M, Amani F, Jafari-Koshki T. Epidemiologic trend of smear-positive, smear-negative, extra pulmonary and relapse of tuberculosis in Iran (2001–2015): a repeated cross-sectional study. J Res Health Sci. 2017;17(2):e00380.
6. Kaffash A, Shobeiri SS, Pouraslan E, et al. The epidemiology of tuberculosis infection and the Human Development Index (HDI) in Iran between 1990–2021: secondary analysis of the global burden of disease. BMC Infect Dis. 2026;26:995. 10.1186/s12879-026-13148-2.
7. Jafari-Koshki T, Arsang-Jang S, Raei M. Applying spatiotemporal models to study risk of smear-positive tuberculosis in Iran, 2001–2012. Int J Tuberc Lung Dis. 2015;19:469–74. 10.5588/ijtld.14.0459.
8. Kiani B, Raouf Rahmati A, Bergquist R, et al. Spatio-temporal epidemiology of the tuberculosis incidence rate in Iran 2008 to 2018. BMC Public Health. 2021;21:1093. 10.1186/s12889-021-11157-1.
9. Rastegar M, Nazar E, Shakeri MT, et al. Spatial distribution of smear-positive pulmonary tuberculosis incidence rates in Iran: a registry-based study (2018–2022). Int J Prev Med. 2024;15:35. 10.4103/ijpvm.ijpvm_346_23.
10. Khodadoust B, Sarvi F, Rimaz S, Khodadost M, Nasehi M. Spatio-temporal analysis of tuberculosis prevalence in Iran. BMC Infect Dis. 2026;26:545. 10.1186/s12879-026-12760-6.
11. Alavi SM, Enayatrad M, Cheraghian B, Amoori N. Incidence trend analysis of tuberculosis in Khuzestan Province, southwest of Iran: 2010–2019. Glob Epidemiol. 2023;6:100118. 10.1016/j.gloepi.2023.100118.
12. Eltayeb D, Pietersen E, Engel M, Abdullahi L. Factors associated with tuberculosis diagnosis and treatment delays in Middle East and North Africa: a systematic review. East Mediterr Health J. 2020;26:477–86. 10.26719/2020.26.4.477.
13. Teo AKJ, Singh SR, Prem K, et al. Duration and determinants of delayed tuberculosis diagnosis and treatment in high-burden countries: a mixed-methods systematic review and meta-analysis. Respir Res. 2021;22:251. 10.1186/s12931-021-01841-6.
14. Nasehi M, Hassanzadeh J, Rezaianzadeh A, et al. Diagnosis delay in smear positive tuberculosis patients. J Res Med Sci. 2012;17:1001–4.
15. Duan Y, Sun M, Cheng C, et al. Tuberculosis patients' delay in healthcare access and its associated factors in Shandong Province, China. BMC Public Health. 2025;25:3729. 10.1186/s12889-025-25090-0.

16. World Health Organization. WHO consolidated guidelines on tuberculosis. Module 3: diagnosis. Geneva: World Health Organization; 2025.
17. World Health Organization. WHO consolidated guidelines on tuberculosis. Module 4: treatment and care. Geneva: World Health Organization; 2025.
18. WorldPop. Global1 2000–2020: unconstrained individual countries 2000–2020 (1 km resolution). University of Southampton. https://hub.worldpop.org/Global1_2000-2020. Accessed 21 Aug 2026.
19. Clayton D, Kaldor J. Empirical Bayes estimates of age-standardized relative risks for use in disease mapping. Biometrics. 1987;43:671–81. 10.2307/2532003.
20. Moran PAP. Notes on continuous stochastic phenomena. Biometrika. 1950;37:17–23. 10.1093/biomet/37.1-2.17.
21. Anselin L. Local indicators of spatial association-LISA. Geogr Anal. 1995;27:93–115. 10.1111/j.1538-4632.1995.tb00338.x.
22. Benjamini Y, Hochberg Y. Controlling the false discovery rate: a practical and powerful approach to multiple testing. J R Stat Soc Ser B. 1995;57:289–300. 10.1111/j.2517-6161.1995.tb02031.x.
23. von Elm E, Altman DG, Egger M, et al. The Strengthening the Reporting of Observational Studies in Epidemiology (STROBE) statement: guidelines for reporting observational studies. PLoS Med. 2007;4:e296. 10.1371/journal.pmed.0040296.
24. Fallahi MJ, Nazemi M, Zeighami A, Shahriarirad R. Changes in incidence and clinical features of tuberculosis with regard to the COVID-19 outbreak in Southern Iran. BMC Infect Dis. 2024;24:1043. 10.1186/s12879-024-09947-0.
25. Mohammadzadeh KA, Ghayoomi A, Maghsoudloo D. Evaluation of factors associated with failure of tuberculosis treatment under DOTS in northern Islamic Republic of Iran. East Mediterr Health J. 2016;22:87–94. 10.26719/2016.22.2.87.
26. Behnaz F, Mohammadzadeh M, Mohammadzade G. Five-year assessment of time of sputum smears conversion and outcome and risk factors of tuberculosis patients in central Iran. Tuberc Res Treat. 2015;2015:609083. 10.1155/2015/609083.
27. Golsha R, Mazandarani M, Sohrabi A, et al. Risk factors and treatment outcome of smear positive pulmonary tuberculosis patients: a five-year study in the North of Iran. Casp J Intern Med. 2024;15:347–53. 10.22088/cjim.15.2.347.
28. Sharafi M, Narouee S, Rasoulizadeh F, et al. Factors associated with survival of tuberculosis patients in Southeast Iran: comparison of stepwise Cox regression, survival tree, and random survival forest. BMC Public Health. 2025;25:3504. 10.1186/s12889-025-24603-1.
29. Jain R, Gupta G, Mitra DK, Guleria R. Diagnosis of extra pulmonary tuberculosis: an update on novel diagnostic approaches. Respir Med. 2024;225:107601. 10.1016/j.rmed.2024.107601.

Figures

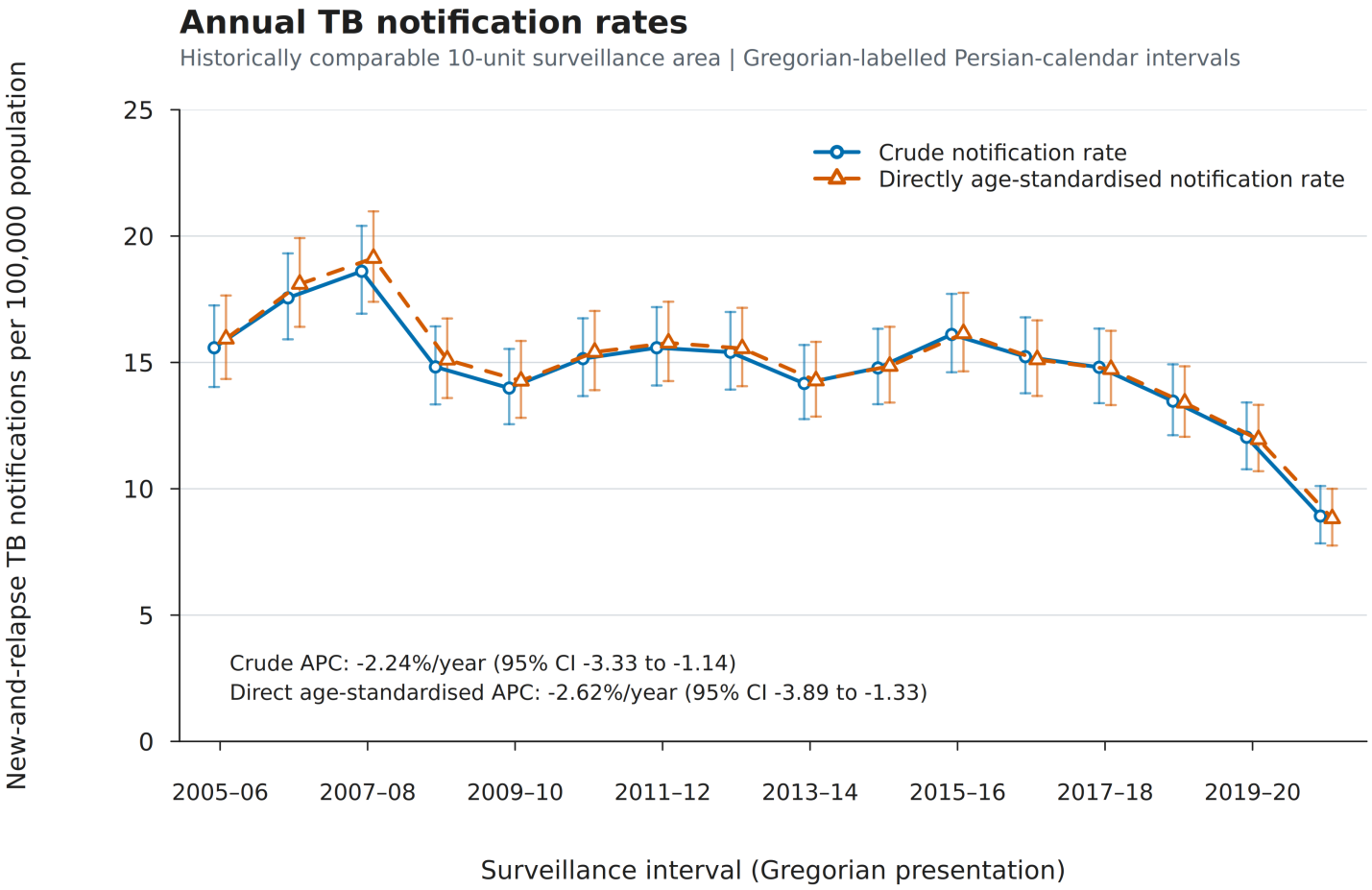


Figure 1

Annual tuberculosis notification rates in the historically comparable surveillance domain. Crude and directly age-standardised new-and-relapse TB notification rates per 100,000 population are shown for the fixed 10-unit domain across the 16 surveillance intervals corresponding to 2005–06 through 2020–21. Points represent annual rates and lines show temporal patterning. The primary model-standardised age-adjusted temporal estimate is reported in the text and Table 2; the direct age-standardised series shown here is a confirmatory analysis.

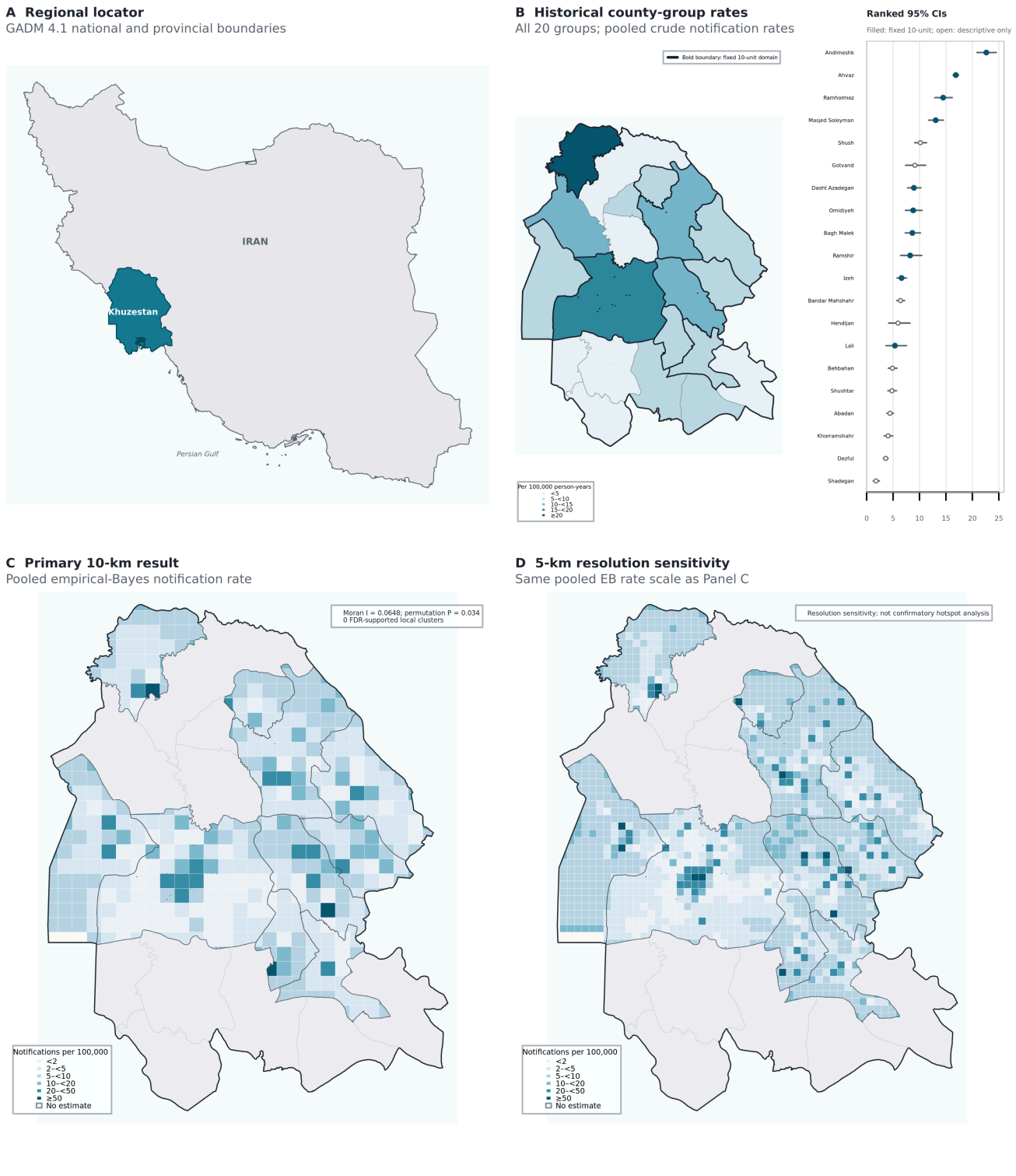


Figure 2

Geographic context and pooled spatial patterns of tuberculosis notification. Panel A locates Khuzestan within Iran. Panel B shows pooled crude new-and-relapse notification rates across all 20 harmonised historical county groups; the fixed 10-unit longitudinal domain is distinguished for context. Panel C presents empirical-Bayes-smoothed pooled notification rates in the primary 10-km grid, and Panel D

shows the nested 5-km resolution sensitivity analysis. Spatial displays use aggregated residence-linked data and do not show individual patient locations. TB, tuberculosis; EB, empirical Bayes.

Supplementary Files

This is a list of supplementary files associated with this preprint. Click to download.

- GraphicalAbstract.tiff